R. L. Garber, J. Wirz, A. Kuroiwa, W. Gehring, *ibid.* **37**, 403 (1984).
12. A. Kishimoto *et al.*, *J. Biol. Chem.* **260**, 12492 (1985); J. R. Woodgett, K. L. Gould, T. Hunter, *Eur. J. Biochem.* **161**, 177 (1986); P. R. Vulliet, F. L. Hall, J. P. Mitchell, D. G. Hardie, *J. Biol. Chem.* **264**, 16292 (1989).
13. M. Rechsteiner, in *Advances in Enzyme Regulation*, G. Weber, Ed. (Pergamon, New York, 1988), vol. 27, pp. 135–151; S. Rogers, R. Wells, M. Rechsteiner, *Science* **234**, 364 (1986).
14. D. A. Melton *et al.*, *Nucleic Acids Res.* **12**, 7035 (1984).
15. K. Johansen, R. Fehon, S. Artavanis-Tsakonas, *J. Cell Biol.* **109**, 2427 (1989); S. Kidd, M. Baylies, G. Gasic, M. Young, *Genes Dev.* **3**, 1113 (1989).
16. Quantitative analysis was performed with a laser densitometer (Pharmacia LKB) and AMBIS software (San Diego). Exposures were chosen that were within the linear response range of the film and the values were normalized to the control RNAs.
17. P. D. Nieuwkoop and J. Faber, *Normal Table of Xenopus laevis* (North-Holland, Amsterdam, 1967).
18. R. Cagan and D. Ready, *Genes Dev.* **3**, 1099 (1989).
19. J. G. Holleyfield, *Dev. Biol.* **18**, 163 (1968).
20. Nucleotide and amino acid sequence information is available through GenBank accession number M33874.
21. J. Devereux, P. Haeberli, O. Smithies, *Nucleic Acids Res.* **12**, 387 (1984).
22. C. R. Kintner and D. A. Melton, *Development* **99**, 311 (1987).
23. J. Dixon and C. Kintner, *ibid.* **106**, 749 (1989).
24. D. A. Melton, *Nature* **328**, 80 (1987).
25. P. Krieg, S. Varnum, W. Wormington, D. A. Melton, *Dev. Biol.* **133**, 93 (1989).
26. T. Maniatis, E. Fritsch, J. Sambrook, *Molecular Cloning: A Laboratory Manual* (Cold Spring Harbor Laboratory, Cold Spring Harbor, NY, 1982), p. 447.
27. We thank S. Artavanis-Tsakonas, J. Campos-Ortega, and E. Knust for providing the *Drosophila Notch* and *Delta* DNAs, A. Newman for technical assistance, D. Ades for the densitometry scans, and C. Holt, G. Lemke, and J. Thomas for critical reading of the manuscript. We gratefully acknowledge support from the NIH and March of Dimes. C.K. is a research fellow of the McKnight and Sloan Foundations.

12 April 1990; accepted 18 June 1990

Calmodulin Activation of Calcium-Dependent Sodium Channels in Excised Membrane Patches of *Paramecium*

Y. SAIMI* AND K.-Y. LING

Calmodulin is a calcium-binding protein that participates in the transduction of calcium signals. The electric phenotypes of calmodulin mutants of *Paramecium* have suggested that the protein may regulate some calcium-dependent ion channels. Calcium-dependent sodium single channels in excised patches of the plasma membrane from *Paramecium* were identified, and their activity was shown to decrease after brief exposure to submicromolar concentrations of calcium. Channel activity was restored to these inactivated patches by adding calmodulin that was isolated from *Paramecium* to the cytoplasmic surface. This restoration of channel activity did not require adenosine triphosphate and therefore, probably resulted from direct binding of calmodulin, either to the sodium channel itself or to a channel regulator that was associated with the patch membrane.

CALMODULIN (CaM) PARTICIPATES in signal transduction processes in most cells. In particular, CaM regulates the activation of certain calcium (Ca^{2+})-dependent potassium (K^+) channels (*1, 2*), the inhibition of the Ca^{2+}-release channel activity of the sarcoplasmic reticulum (*3*), and, perhaps, the gap junction channel (*4*). However, the mechanism by which CaM regulates ion channel activity is not well understood. CaM may interact directly with channel proteins, as suggested in cell-free systems (*2, 3*) or may affect channel activity through Ca^{2+}, CaM-dependent covalent modifications of the channel proteins (*5*). In addition, CaM may control transcription of genes, as suggested in plants (*6*), possibly including those that encode ion channels.

CaM regulates ion channels in *Paramecium*. Mutations in the CaM structural gene eliminate one or more of three Ca^{2+}-dependent ion currents recorded under whole-cell voltage clamp (*7*). To decipher the mechanism of CaM regulation of ion channels in *Paramecium*, we used a patch-clamp technique to study Ca^{2+}-dependent sodium (Na^+) single channels in excised patches from *Paramecium*.

Previous studies with whole-cell *Paramecium* have shown that activation of the Na^+ conductance is dependent on cytoplasmic, free Ca^{2+}, and that the Na^+ channel is permeable to Na^+ and lithium (Li^+), but not potassium (K^+) or cesium (Cs^+) (*8*); similar conductances have been found in other organisms (*9*). With 100 mM Na^+ in both pipette and bath (*10*), patch-clamp recordings (*11*) revealed single-channel activities (Fig. 1A) in excised inside-out patches of the plasma membrane from *P. tetraurelia* (*12*) when 10^{-5} M free Ca^{2+} was present in the bath (on the cytoplasmic side of the patch). The channel was more active at positive than at negative voltages. The current amplitude, measured from the amplitude histograms, was plotted as a function of membrane voltage (I-V plot), and the conductance was determined to be 19.0 pS [± 3.2 (mean ± standard deviation, SD), n = 10; error limits of ±SD are used throughout the report] (Fig. 1B) (*13*).

The ion selectivity of the channel (*14*) was determined by substitution of Na^+ in the bath with other ions. From I-V plots of single-channel currents under bi-ionic conditions (Fig. 1C) and reversal potential analyses (*15*) (Fig. 1D), we determined the relative permeability ratios of Na^+:Li^+:K^+:Cs^+ to be 1:0.76:0.07:0.05, respectively (n = 3). The conductance and ion selectivity of the Na^+ single channel in *Paramecium* were therefore similar to those of its counterparts in higher organisms, which are voltage- and not Ca^{2+}-gated (*16*).

The Ca^{2+} dependence of the *Paramecium* Na^+ channel was examined by changing the free Ca^{2+} concentration of the bath. After measuring the channel activity at 10^{-5} M Ca^{2+} (Fig. 2A, left), the bath was perfused with a solution of 10^{-8} M Ca^{2+}, and the channel activity at all voltages fell nearly to zero (Fig. 2A, middle). This suggested that the channel activity was Ca^{2+} dependent. However, a return to 10^{-5} M Ca^{2+} after brief exposure to 10^{-8} M Ca^{2+} failed to restore channel activity (Fig. 2A, right). The initial activity at 10^{-5} M Ca^{2+} was reduced upon returning to 10^{-5} M Ca^{2+} after exposure to 10^{-8} M Ca^{2+} for 60 s [1.19 ± 1.04 versus 0.08 ± 0.12, expressed as the activity of all channels in the patch (NPo) at −50 mV, n = 6; 60 to 150 s elapsed between the two measurements] (*17*). By contrast, continuous exposure to 10^{-5} M Ca^{2+} for similar durations (Fig. 2B) did not alter channel activity, which varied from 1.20 ± 0.59 to 1.26 ± 0.88 (n = 8, 55 to 175 s elapsed, including a 30- to 140-s perfusion period). However, even at 10^{-5} M Ca^{2+}, the channel activity declined with prolonged exposure (>30 min). These findings suggested that a factor or factors required for Na^+-channel activity was rapidly degraded or inactivated by exposure to 10^{-8} M Ca^{2+}.

Because the Ca^{2+}-dependent Na^+ conductance of *Paramecium* is under the control of calmodulin (CaM) in vivo (*7*), we tested whether CaM, when applied to the cytoplasmic surface of the patch membrane, could restore activity to inactivated Na^+ channels in vitro. When channel activity had declined, we added *Paramecium* CaM (2 μg, >85% pure) (*18*) to the 300-μl bath that contained 10^{-5} M Ca^{2+}. We observed an increase in

Laboratory of Molecular Biology, University of Wisconsin–Madison, Madison, WI 53706.

*To whom correspondence should be addressed.

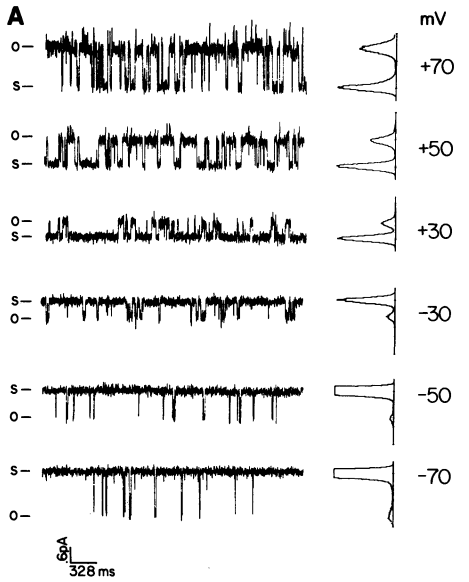

channel activity during a 5-min period of incubation with CaM. However, the channel activity became more pronounced after removal of CaM from the bath, the reason for which is yet to be understood. Thus, incubation with CaM dramatically increased channel activity (0.33 ± 0.47; Fig. 3A, middle) over that observed prior to CaM addition (0.04 ± 0.08, NPo at −50 mV, n = 5; Fig. 3A, left) (*19*). The activity of the channel reactivated with CaM was less than the activity prior to channel inactivation, perhaps due to time-dependent loss of channel activity by an unknown mechanism. However, the channel reactivated by CaM had the same conductance (17.5 ± 1.0 pS, n = 4) as the Ca^{2+}-dependent Na^+ channel, was selective for Na^+ over K^+ (*20*), was dependent on Ca^{2+} (*20*), and lost activity upon exposure to 10^{-8} M Ca^{2+} (Fig. 3A, right). Inactivation and reactivation of the channel could be repeated several times, although the degree of channel reactivation lessened with time. More highly purified *Paramecium* CaM (>98% pure) and bovine CaM (>95% pure) (*21*) were both capable of reactivating the Na^+ channel ($n \geq 3$ for each) (*20*). Ovalbumin from chicken (>98% pure; 10 μg) (*21*) yielded little change in the channel activity (from 0.02 ± 0.03 to 0.04 ± 0.08, at −50 mV, n = 5; Fig. 3B). Similarly, no effect was observed with the Ca^{2+}-binding proteins parvalbumin (>99% pure) and chicken troponin C (>75% pure) (5 μg, n = 3 for each) (*21*). All such experiments with negative results were followed by incubation with *Paramecium* CaM and confirmed that the Na^+ channel could be reactivated.

Channel activity can be modulated by phosphorylation (*22*). However, because reactivation of the Na^+ channel did not require adenosine triphosphate, the CaM effect was probably not mediated by a Ca^{2+}, CaM-dependent protein kinase. This suggests that Ca^{2+} and CaM may activate the channel by binding directly to the channel protein or to another membrane component that in turn activates the channel. Direct interaction between channels and CaM may be widespread; a Ca^{2+}-CaM complex appears to directly inactivate the Ca^{2+}-release channel of sarcoplasmic reticulum (*3*), and CaM binds certain ion-channel proteins in vitro (*2, 23*). The mechanism by which CaM transduces Ca^{2+} signals to the channel may be further elucidated by introducing site-directed mutations into the gene for CaM

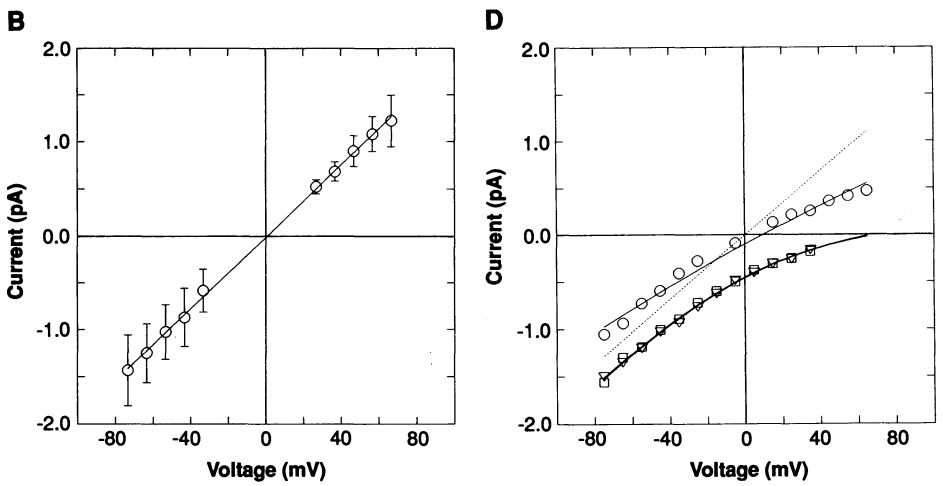

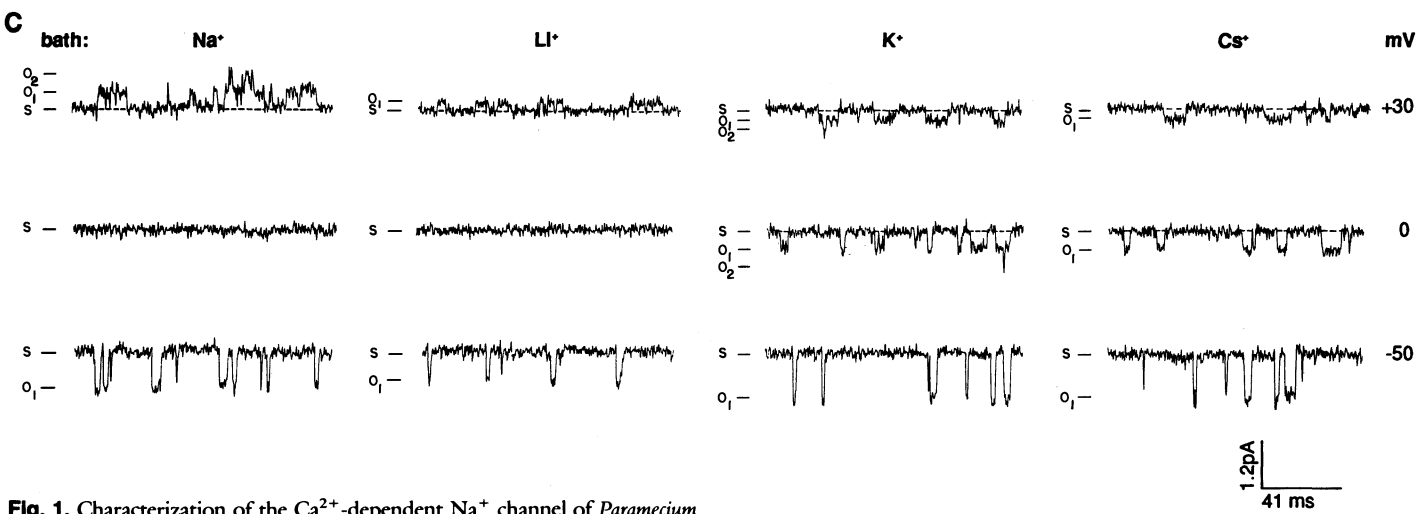

Fig. 1. Characterization of the Ca^{2+}-dependent Na^+ channel of *Paramecium* in excised inside-out patches. (**A**) A family of single-channel currents at voltages indicated at the right of each trace recorded in a symmetric Na^+ solution with 10^{-5} M Ca^{2+} (*10*). On the right are amplitude-distribution histograms from stretches of data (>15 s each) including the portions shown here. Abbreviations for all figures are: s, shut level; o, openings of channels. (**B**) Unit current amplitude-voltage relation in the symmetric Na^+ solution, showing means ± SD from ten patches. The result of linear regression with a slope of 19 pS is also drawn. (**C**) Ion selectivity of the Na^+ channel. The pipette contained 100 mM Na^+ and the bath contained 100 mM of Na^+, Li^+, K^+, or Cs^+, as indicated (*10, 14*). Therefore, inward currents were carried by Na^+ and outward currents by Na^+ or other substituting ions in the bath. Membrane voltages are indicated beside the traces. o_1, one opening; o_2, two openings. (**D**) I-V relations in different ion solutions from the same patch shown in (**C**). ○, Li^+; ▽, K^+; and □, Cs^+. The data were fitted to the GHK equation (*15*), and the best-fit results are represented by lines drawn through symbols. The dashed line indicates results for Na^+.

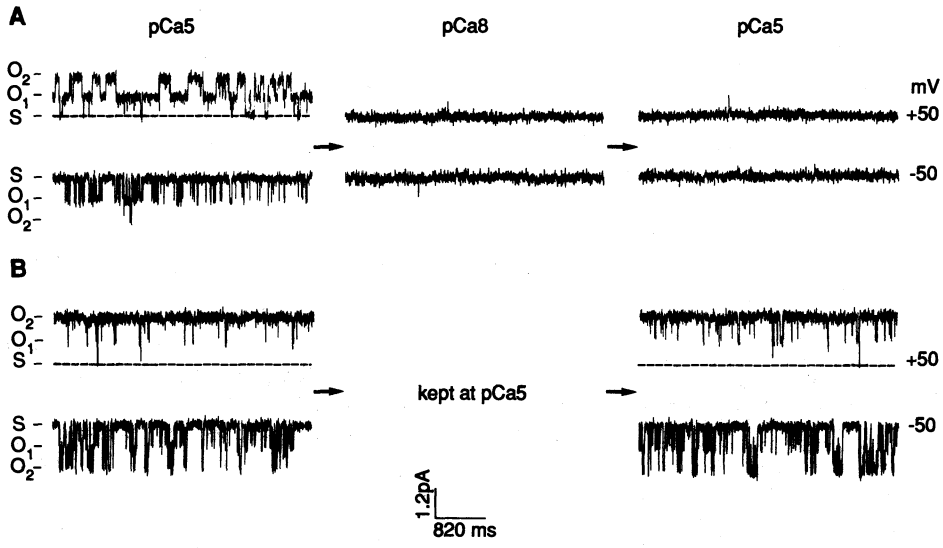

Fig. 2. Ca^{2+} dependence and inactivation of the Na^+ channel. (**A**) The channel activity in the Na^+ solution was recorded first with 10^{-5} M Ca^{2+} (pCa5, left) and then at 10^{-8} M Ca^{2+} (pCa8, middle). After a 60-s exposure to 10^{-8} M Ca^{2+}, the bath was perfused with 10^{-5} M Ca^{2+}, and the channel activity was again recorded (pCa5, right). Voltages are indicated beside the traces. (**B**) A control experiment with a different patch, showing that the Na^+ channel activity changed little after superfusing the patch with 10^{-5} M Ca^{2+} for >70 s.

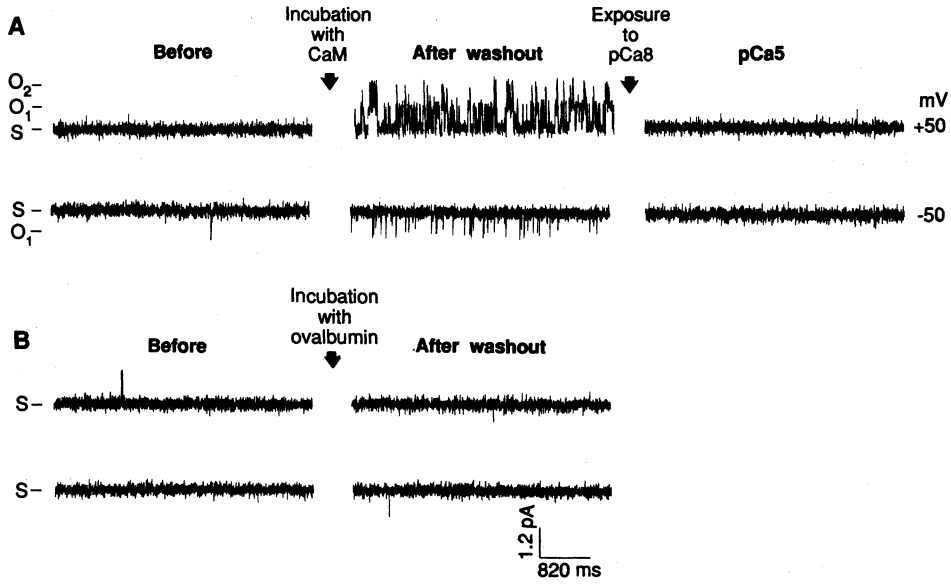

Fig. 3. Reactivation of the Na^+ channel by CaM. (**A**) When the channel became inactive (before, left), *Paramecium* CaM (2 μg, 0.4 μM) (*18*) was added to the bath that contained the Na^+ solution of 10^{-5} M Ca^{2+}. After a 5-min incubation, CaM was washed out of the bath by perfusing with 10^{-5} M Ca^{2+}. The channel activities upon depolarization and hyperpolarization were recorded (after washout, middle). The patch was then exposed to 10^{-8} M Ca^{2+} for 60 s, and returned to 10^{-5} M Ca^{2+}. The subsequent channel activity was recorded at 10^{-5} M Ca^{2+} (pCa5, right). (**B**) In a control experiment, ovalbumin (10 μg, 0.8 μM) (*21*) was added to the bath that contained 10^{-5} M Ca^{2+}. The patch was incubated for 5 min and then superfused with 10^{-5} M Ca^{2+}. The channel activity changed only slightly [compare left panel (before) to right (after)].

and testing the ability of the mutant protein to activate the Ca^{2+}-dependent Na^+ channel of *Paramecium* (*7*).

REFERENCES AND NOTES

1. L. Pape and B. I. Kristensen, *Biochim. Biophys. Acta* **770**, 1 (1984); H. A. Pershadsingh, R. D. Gale, D. M. Delfert, J. M. McDonald, *Biochem. Biophys. Res. Commun.* **135**, 934 (1986); M. Onozuka, H. Furuichi, K. Kishi, S. Imai, *Comp. Biochem. Physiol.* **86A**, 589 (1987); Y. Okada, T. Yada, T. Ohno-Shosaku, S. Oiki, *J. Membr. Biol.* **96**, 121 (1987); V. N. Serebryakov, P. D. Bregestosvski, V. L. Zamoyski, J. Stinnakre, *Pflügers Arch.* **414**, S185 (1989); but also see the case without a CaM effect by E. S. Levitan and I. B. Levitan, *J. Membr. Biol.* **90**, 59 (1986).
2. D. A. Klaerke, J. Petersen, P. L. Jørgensen, *FEBS Lett.* **216**, 211 (1987).
3. G. Meissner and J. S. Henderson, *J. Biol. Chem.* **262**, 3065 (1987); J. S. Smith, E. Rousseau, G. Meissner, *Circ. Res.* **64**, 352 (1989).
4. C. Peracchia and S. J. Girsch, *Am. J. Physiol.* **248**, H765 (1985); C. Peracchia, in *Cell Interactions and Gap Junctions*, N. Sperelakis and W. C. Cole, Eds. (CRC Press, Boca Raton, FL, 1989), vol. 1, pp. 125–142; but also see D. C. Spray and M. V. L. Bennett, *Annu. Rev. Physiol.* **47**, 281 (1985).
5. J. Acosta-Urquidi, D. L. Alkon, J. T. Neary, *Science* **224**, 1254 (1984); J. E. Chad and R. Eckert, *J. Physiol.* **378**, 31 (1986); M. Sakakibara *et al.*, *Biophys. J.* **50**, 319 (1986).
6. J. Braam and R. W. Davis, *Cell* **69**, 357 (1990).
7. R. D. Hinrichsen, A. Burgess-Cassler, B. C. Solvedt, T. Hennessey, C. Kung, *Science* **232**, 503 (1986); R. R. Preston, M. A. Wallen-Friedman, Y. Saimi, C. Kung, *J. Membr. Biol.* **115**, 51 (1990) ; K.-Y. Ling *et al.*, *FASEB J.* **4**, A620 (1990); J. A. Kink *et al.*, *Cell* **62**, 165 (1990). Three of the CaM gene mutations, cam^1, cam^2, and cam^3, nearly eliminate two separate Ca^{2+}-dependent K^+ currents, but the Ca^{2+}-dependent Na^+ current is only slightly affected by the mutations. The effects on these currents are reversed in cam^{11}, cam^{12}, and cam^{13}.
8. Y. Saimi, *J. Membr. Biol.* **92**, 227 (1986).
9. L. A. Jaffe, R. T. Kado, D. Kline, *J. Physiol.* **381**, 263 (1986); T. Krüppel and W. Lueken, *J. Membr. Biol.* **116**, 79 (1990).
10. All of the Na^+ solutions in this report consisted of 100 mM Na^+, 5 mM Hepes, 0.01 mM EDTA, 20 mM Cl^-, and ~ 80 mM glutamate (pH ~7.0, adjusted with glutamic acid), as well as 10^{-4} to 10^{-8} M free Ca^{2+} buffered by 1 mM EGTA. The free Ca^{2+} concentration was calculated assuming an apparent association constant of EGTA to be $10^{6.68}$ (*12*). The pipette was filled with the Na^+ solution of 10^{-5} M Ca^{2+}. All the bath solutions contained 10^{-4} to 10^{-8} M free Ca^{2+} with 1 mM dithiothreitol in the Na^+ solution. In the ion-selectivity experiments, 100 mM Na^+ in the bath was substituted with equimolar Li^+, K^+, or Cs^+ in the presence of 10^{-4} or 10^{-5} M Ca^{2+}. An agar bridge with 3 M KCl was used as a reference electrode (*12*). All experiments, conducted between 20° and 23°C, were repeated on three or more patches. Statistics are given as means ± SD.
11. O. P. Hamill, A. Marty, E. Neher, B. Sakmann, F. J. Sigworth, *Pflügers Arch.* **391**, 85 (1981).
12. Because patch clamping of live *Paramecium* proved to be difficult, we developed a method to isolate its surface membrane [Y. Saimi and B. Martinac, *J. Membr. Biol.* **112**, 79 (1989)]. Briefly, paramecia were incubated in 100 to 150 mM sodium glutamate, 10^{-5} M free Ca^{2+}, 5 mM Hepes (pH ~7.0) to induce blisters (typically ≤20 μm in diameter) on the body surface membrane. These blisters were detached from the body and put in the solution for giga-seal formation (*10*). The blister membrane probably consisted of the cell body membrane and a small amount of other membranes, including cilia.
13. An offset of +3.3 (±2.1 mV, n = 10) was detected in the symmetric Na^+ solution of 10^{-5} M Ca^{2+} and was corrected for throughout this report.
14. Although patches with only the Na^+ channel (mean open time, 4 to 64 ms) were used primarily for the ion-selectivity study, two other channel types were present and dealt with as follows. A nonselective cation channel (>20 pS, Ca^{2+}-independent, strongly depolarization-dependent, mean open time <2 ms) was partially suppressed by 3 to 10 μM tetrapentylammonium, which affected only slightly the measurements of the Na^+ conductance at 100 μM. The Ca^{2+}-dependent K^+ channel (*12*) was silent in the absence of K^+.
15. The Goldman-Hodgkin-Katz (GHK) equation below was used to fit data in the presence of alkali matal ions:

$$i = \frac{\alpha F^2 E[1 - \exp\{-(E - E_r)F/RT\}]}{RT[1 - \exp(-EF/RT)]}$$

where i is the current amplitude through the channel, E the voltage across the membrane, F the Faraday constant, T absolute temperature, and R the gas constant. The best-fit curves for Na^+, Li^+, K^+, and Cs^+ (Fig. 1D) were drawn with reversal potentials (E_r) of 0.04×10^{-3}, 9.26×10^{-3}, 70.2×10^{-3}, and 67.5×10^{-3}, and constants (α) of 4.47×10^{-6}, 2.31×10^{-6}, 0.31×10^{-6}, and 0.34×10^{-6}, respectively. The calculated E_r's (n = 3) in the presence of Li^+, K^+, and Cs^+ were (in

millivolts) +7.0 ± 2.2, +66.7 ± 6.2, and +76.0 ± 11.6, respectively. Data points for Li^+, however, did not fit well to the GHK equation (the real E_r appeared to be more negative); this and strong rectification upon depolarization may suggest blockage of the channel by Li^+. Channel blockage by permeant ions has been described [D. J. Adams, W. Nonner, T. M. Dwyer, B. Hille, *J. Gen. Physiol.* **78**, 593 (1981); S. Cukierman, G. Yellen, C. Miller, *Biophys. J.* **48**, 477 (1985); G. Eisenman, R. Latorre, C. Miller, *ibid.* **50**, 1025 (1986)].

16. B. K. Krueger, J. F. Worley III, R. J. French, *Nature* **303**, 172 (1983); S. Garber and C. Miller, *J. Gen. Physiol.* **89**, 459 (1987).
17. The channel activity (NPo) was derived from data >15 s either by multi-channel dwell time analyses or by amplitude histogram analyses. For the purpose of describing the activity of an unspecified number of channels, NPo is equal to the product of the number of channels and the probability of channel opening.
18. Wild-type CaM from *Paramecium* was prepared according to the method of T. J. Lukas, M. A. Wallen-Friedman, C. Kung and D. M. Watterson [*Proc. Natl. Acad. Sci. U.S.A.* **86**, 7331 (1989)], with minor modifications. The CaM concentration in *Paramecium* is estimated to be ~1 pg per 200 pl, or 0.3 μM [see the first reference of (7)]. Therefore, the concentration of CaM we used in this report was very close to the physiological concentration.
19. Channel reactivation was observed in ~70% of the trials (>20), including ones under slightly different conditions.
20. Y. Saimi and K.-Y. Ling, unpublished data. The identity of reactivated channels with respect to conductance, and selectivity for Na^+ over K^+, and Ca^{2+} dependence was confirmed in at least three experiments.
21. Chicken ovalbumin, bovine CaM, and rabbit parvalbumin were salt-free preparations (Sigma). Chicken troponin C (~75% pure) was a gift of M. Sundaralingam.
22. L. K. Kaczmarek and I. B. Levitan, in *Neuromodulation* (Oxford Univ. Press, New York, 1987), p. 286.
23. E. Hertzberg and N. B. Gilula, *Cold Spring Harbor Symp. Quant. Biol.* **46**, 639 (1981); M. J. Welsh, J. C. Aster, M. Ireland, J. Alcala, H. Maisel, *Science* **216**, 642 (1982); L. J. Van Eldik, E. L. Hertzberg, R. C. Berdan, N. B. Gilula, *Biochem. Biophys. Res. Commun.* **126**, 825 (1985).
24. We thank C. Kung, P. V. Minorsky, and R. R. Preston for their comments on this report and R. Burns for technical support. Supported by NIH grants GM22714 and GM36386, and the Lucille P. Markey Charitable Trust.

2 May 1990; accepted 12 July 1990

Birth of Projection Neurons in Adult Avian Brain May Be Related to Perceptual or Motor Learning

ARTURO ALVAREZ-BUYLLA, JOHN R. KIRN, FERNANDO NOTTEBOHM

Projection neurons that form part of the motor pathway for song control continue to be produced and to replace older projection neurons in adult canaries and zebra finches. This is shown by combining [^{3}H]thymidine, a cell birth marker, and fluorogold, a retrogradely transported tracer of neuronal connectivity. Species and seasonal comparisons suggest that this process is related to the acquisition of perceptual or motor memories. The ability of an adult brain to produce and replace projection neurons should influence our thinking on brain repair.

THE SONG CONTROL SYSTEM OF OSCINE songbirds consists of several discrete nuclei including the high vocal center (HVC) and the robust nucleus of the archistriatum (RA) (*1*). These two brain regions form the backbone of the telencephalic efferent pathway that controls learned song. HVC is remakable in that new neurons continue to be added to it in adulthood (*2, 3*).

HVC includes two types of projection neurons: those that project to area X and those that project to RA (*1, 3*). Area X–projecting HVC neurons are produced during early development (*4*), as is also true for projection neurons in the brains of most warm-blooded vertebrates (*5*). In contrast, the majority of RA-projecting HVC neurons are added after hatching (*4, 6*). According to previous reports, the latter process slows down by the time birds reach sexual maturity (*4, 6*). We now explore the extent to which new RA-projecting neurons continue to be added to the adult HVC.

Twelve adult male canaries received injections of [^{3}H]thymidine (*7*), a marker of DNA synthesis, twice daily for 14 days. One-hundred and twenty-five days later (*8*), we injected fluorogold into the right and left nucleus RA by using stereotactic coordinates (*4*). These birds were killed 4 days later and their brains sectioned at 6-μm intervals; the sections were prepared for autoradiography and counterstained for anatomical detail (*9*). We scored the position and number of (i) neurons, (ii) fluorogold-backfilled neurons, (iii) [^{3}H]thymidine-labeled neurons, and (iv) double-labeled neurons (fluorogold plus [^{3}H]thymidine) within HVC with a computer-yoked microscope (*10*).

The cell bodies of HVC neurons backfilled with fluorogold stand out unambiguously from surrounding neuropil (Fig. 1A). Fluorogold injections outside, but in the vicinity, of RA failed to label HVC neurons. HVC cells backfilled from RA with fluorogold fall into a rather homogeneous size class [nuclear diameters of 6.18 ± 0.58 (mean ± SD)] and are generally smaller than area X–projecting cells (*3, 4*). The RA-projecting neurons constituted 54% of HVC neurons (*11*).

Many of the fluorogold-backfilled HVC neurons had nuclei labeled with [^{3}H]thymidine (Fig. 1B), indicating that they were born at the time of [^{3}H]thymidine treatment (*12*). Thus, some of the canary HVC neurons generated in adulthood became RA-projecting cells. Previous work in which horseradish peroxidase was used as a retrograde label in adult male canaries revealed very few new RA-projecting HVC neurons, and it was concluded that adult HVC neurogenesis was restricted almost exclusively to the formation of interneurons (*3*). Therefore, in our study we had to rule out the possibility that fluorogold transported retrogradely from RA to HVC passed from projection neurons to interneurons. We injected nucleus RA of an additional five adult male canaries with fluorescent rhodamine beads; these birds were killed 4 days later. Beads are trapped in intracellular organelles and do not leak out of the cell even after long survivals (*13*). The birds had been treated with [^{3}H]thymidine (*7*) and tissue was processed to preserve the fluorescent beads (*14*). Neurons double-labeled with silver grains over their nuclei and beads in their cytoplasm (Fig. 1, C and D) were found in all five canaries. These observations confirm that RA-projecting HVC neurons continue to be generated in adult canary brain.

Adult male canaries learn new songs seasonally (*15, 16*). To address the possible relationship between adult neurogenesis and song plasticity, we injected some canaries with [^{3}H]thymidine in May, when song is stable, and some in October, when song is modified (*7*). The percentage of HVC neurons that were [^{3}H]thymidine labeled was 4.9 times higher in the October group (mean, 3.8%; range, 1.6 to 6.1%) than in the May group (mean, 0.78%; range, 0.23 to 1.5%) (Fig. 2, a and b). Nevertheless, in both the May and October groups, more than half of the new neurons were backfilled with fluorogold (56% and 71%, respectively). Therefore, there were correspondingly more RA-projecting HVC neurons labeled with [^{3}H]thymidine in the October group than in the May group (Fig. 2, a and b). Moreover, in 4-year-old canaries injected with [^{3}H]thymidine in October, the number of new RA-projecting HVC neurons was also considerably higher than in the 1-year-old May group (Fig. 2, a to c) (*17*). Because of the 4-month delay between [^{3}H]thymidine administration and the time when the birds were killed, we do not know whether the lower numbers of new RA-projecting HVC neurons after [^{3}H]thymi-

The Rockefeller University Field Research Center, Tyrrel Road, RR2, Box 38B, Millbrook, NY 12545.